

## Molecular insights into 5-hydroxy-1-methoxyxanthone reactivity, stability and antidiabetic activity in green solvents

Mohamed Hisam Rasheed Ahmed<sup>1</sup>, Ramanujam Girija<sup>2</sup>, Muthiyam Lawrence<sup>2</sup>, Sathiyadhas Sahaya Jude Dhas<sup>3\*</sup>, Loganathan Bhuvaneshwari<sup>4</sup>, Rajesh Punniamorthy<sup>1\*</sup>, Anbarasu Mariyappillai<sup>5</sup> & Kayashrini Sundaramoorthi<sup>1</sup>

<sup>1</sup>Department of Physics, Vels Institute of Science, Technology and Advanced Studies, Pallavaram, Chennai-600 117, Tamil Nadu, India

<sup>2</sup>Department of Physics, Loyola Institute of Technology, Palanchur, Chennai-600 123, Tamil Nadu, India

<sup>3</sup>Saveetha School of Engineering, Saveetha Institute of Medical and Technical Sciences, Saveetha University, Chennai-602 105, Tamil Nadu, India

<sup>4</sup>Department of Physics, N.K.R. Govt. Arts College for Women, Namakkal-637 001, Tamil Nadu, India

<sup>5</sup>Department of Agronomy, School of Agriculture, Vels Institute of Science and Technology & Advanced Studies, Pallavaram, Chennai-603 203, Tamil Nadu, India

Received 29 May 2025; revised 24 March 2026

Using combined pharmacological and computational methods, this study seeks to assess the therapeutic potential of 5-Hydroxy-1-Methoxyxanthone (5H1MX) while encouraging the use of green solvents. In order to verify molecule stability, intramolecular charge transfer, hyperconjugation, and stabilization energy were examined using Natural Bond Orbital (NBO) analysis. Density Functional Theory (DFT) techniques were used to examine the Mulliken charge distribution and Molecular Electrostatic Potential (MEP). Chemical reactivity was predicted and reactive spots were identified using Fukui functions and global descriptors. The  $C_{13}-C_{17}$  to  $C_{12}-C_{15}$  ( $\pi^*$ ) interaction was found to have the highest stabilization energy of 472.42 kcal/mol. The gas phase had the largest band gap value (4.179 eV) among the environments under study. Using several green solvents, solvent effects were investigated, and the results showed a considerable impact on molecular characteristics and reactivity. The system's electrical behavior was further validated using ELF, LOL, and RDG investigations. In accordance with Lipinski's rule of five, positive pharmacological features were validated by drug-likeness measures and NMR analysis. Strong binding affinity for the target protein was shown by molecular docking data, indicating that 5H1MX is a viable option for antidiabetic applications.

**Keywords:** *Arenaria serpyllifolia* L., DFT, Fukui function, IEFPCM, Multiwave function

In contemporary chemical and medical research, a search for strong medicinal agents and ecologically safe solvents has grown in importance in contemporary chemical and medical research. In this regard, the incorporation of quantum mechanical techniques offers an effective method for deciphering the intricate interactions inside molecular systems and forecasting their behavior in different scenarios. This work is centered on a thorough investigation of Molecular Docking, Electrostatic, and Drug likeness, and molecular structure of various green solvents, as well as pharmacological studies of 5-Hydroxy-1-Methoxyxanthone ( $C_{14}H_{10}O_4$ ), a compound of great interest because of its anti-diabetic properties. G. Don explained in the literature that a natural substance isolated from *Mammea Africana* and the synthetic

5-hydroxy-1-methoxy xanthone were similar (Found: C, 69.2; H, 4.2. C & 1, 4 requires C, 69.4; H, 4.1%)<sup>1</sup>. As of a dichloromethane extract of the stem and roots of *Hypericum brasiliense*, four novel  $\gamma$ -pyrone (hyperbrasilone), three known xanthones (1, 5-dihydroxy xanthone, 5-hydroxy-1-methoxyxanthone and 6-deoxyjacareubin) thereby betulinic acid were obtained. The xanthones and Hyperbrasilone exist in all antifungals against *Cladosporium cucumerinum*<sup>2,3</sup>. The bark of the Myanmar-native *Kaya aassamica* (Clusiaceae) was used to extract coumarin derivatives called theraphins (5-hydroxy-1-methoxyxanthone). Chemical and spectroscopic methods were utilized to establish their structures. Theraphin's only action against the KB cell line was minimal. The coumarins also showed a small amount of antimalarial activity. Two novel xanthones were extracted from the stem of *Poeciloneuron pauciflorum*. In addition to the two well-known xanthones (1, 5-dihydroxy- and 5-

\*Correspondence:

E-mail: judedhas@gmail.com, rajesh.ncc5coy@gmail.com

hydroxy-1-methoxyxanthone) and (-)-epicatechin, a novel xanthone (2, 7-dihydroxyxanthone) was recovered in the aerial portions (bark and stem) of *Mammea acuminata* which has biological uses<sup>4,5</sup>.

Demand for novel antimalarial drugs is sparked by the evolution of antimalarial medication resistance. The medicinal herb *Mammea siamensis*, a member of the Calophyllaceae family, is utilized in several traditional Thai dishes. There are 13 chemicals in this plant, including the title compound, which has been proven to have strong antimalarial action. Therefore, the purpose of this work was to separate active substances from *M. siamensis* flowers and assess their potential for treating malaria<sup>6</sup>. 5-hydroxy-1-methoxyxanthone was extracted from *Arenaria serpyllifolia* L by solvent fractionation and subsequent separations with silica gel, ODS, Sephadex LH-20 and semi-preparative HPLC chromatography and their structures were characterized by spectroscopic investigation and identified<sup>7</sup>. A significant medicinal plant called *Arenaria serpyllifolia* L. grows in the subtropical and temperate Himalayan areas from Nepal to Kashmir. Traditional medicine makes use of plants to heal renal and bladder-related issues. Density functional theory (DFT) computations for the molecular structure and reactivity are performed, and topological studies are used to forecast the electron density distribution. A molecular Electrostatic Potential (MEP) investigation is carried out to reveal the molecular locations that are vulnerable to chemical assault. Particular target proteins are used for docking. Similar investigations conducted by other research groups demonstrated that these theoretical analyses offer an early understanding of the nature, reaction, and powerful therapeutic potential of organic substances in biological structures. Applying techniques based on deep learning to predict molecular characteristics like lipophilicity is another way to predict bioactivity and drug-like characteristics. These models are being demonstrated to provide accurate and reliable predictions<sup>8,9</sup>. Water, methanol, ethanol, and acetone were the solvents of choice for researching the influence of solvents on various physical as well as chemical properties. These substances were selected so that the gradation of their characteristics with increasing polarity could be seen. The use of green solvents is preferred since these molecules mostly interact favourably via hydrogen bonds. Since it serves as the surfactant of reaction and distribution in biological systems, water, the most used aqueous solvent, is the medium of most interest in the present work. Investigating the effects of the solvation is done using the continuous model,

IEFPCM<sup>10,11</sup>. It is anticipated that the results will support the creation of chemical and pharmaceutical applications that are more efficient and sustainable, in line with current objectives of environmental stewardship and better health outcomes. A comprehensive investigation integrating quantum chemical analysis, solvent effects utilizing green media, and molecular docking for (5H1MX) is still lacking, despite several research highlighting the biological relevance of xanthone derivatives. Density Functional Theory (DFT), Natural Bond Orbital (NBO) analysis, Fukui function descriptors, and IEFPCM solvation models are all uniquely integrated in this work to assess the compound's reactivity and structure property connection. Additionally, the study focuses on ecologically safe solvents to comprehend their impact on biological and electrical characteristics. By offering fresh perspectives on the stability, reactivity, and antidiabetic potential of 5H1MX, this theoretical and pharmacological approach aids in the creation of long lasting and powerful medication candidates.

### Computational details

Density Functional Theory (DFT) at the B3LYP/6-311++G(d,p) level of theory was used for all quantum chemistry computations<sup>12,13</sup>. The aforementioned source theory level was used for all additional computational, including MEP and FMOs in the gas phase and with selected solvents such as water, methanol, ethanol, and acetone. NBO investigations are being utilized to investigate whether atomic orbitals interact with isolated pairs, bonds, and anti-bonds<sup>14,15</sup>. Using the Swiss ADME online tool results on pharmacological characteristics and lipophilicity were obtained<sup>16</sup>. This work investigated the molecular docking interaction between the analyzed ligand molecule and the target protein using the Auto Dock 4.2.6 set and then assessed it by the Py MOL program<sup>17</sup>.

### Results and Discussion

#### GC-MS analysis

Gas chromatography–mass spectrometry (GC–MS) is a widely used technique for analyzing compounds in liquid, gaseous, and solid samples. The analysis begins with sample vaporization in the gas chromatograph, followed by separation using a capillary column. The chemical composition of Iranian propolis extracts that were collected in 2023 from two provinces in northern Iran: Ardabil and Polur from Mazandaran Province were measured through gas chromatography-mass spectrometry (GC-

MS) methods<sup>18</sup>. In addition, antimicrobial activity and cytotoxicity effects on HN5 and LNCaP cell lines were evaluated. The data were analyzed using one-way ANOVA and  $P < 0.05$  was considered significant. The GC-MS analysis in Figure 1, identifies the presence of compounds that belong to different groups such as aromatics acids and their related esters, flavonoid and flavonoid derivatives and

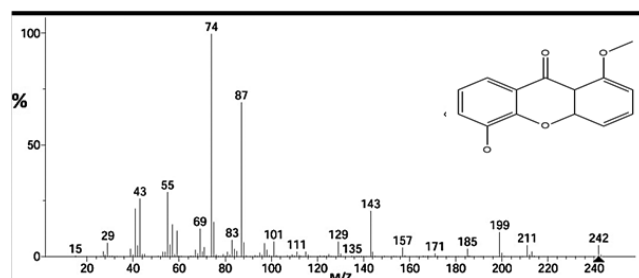


Fig. 1 — GC-MS Chromatogram of 5H1MX molecule

terpenes. Flavanone is the most dominant compound of flavonoids. The maximum growth inhibition is observed against *S. aureus* of ethanolic extract of propolis ( $P < 0.05$ ). Moreover, cytotoxicity shows that ethanolic and dichloromethane extracts have more inhibitory effects on cell lines than the water extract.

#### NBO analysis

NBO analysis is an effective tool for evaluating intermolecular and intramolecular interactions. This analysis is used to study the charge transport and conjugative interactions. The 2<sup>nd</sup> order Fock matrix approach is used to evaluate the links between donor and acceptor atoms in natural bonding analyses. It is feasible to determine the stabilization energies  $E(2)$  is connected to the de-localization of each donor (i) and acceptor (j). The NBO fraction that is off-diagonal is  $F(I,j)$ . In the Fock matrix, the donor filling is represented by the principal diagonals of  $q_i$  and  $E_i^{19,20}$ . Table 1 displays the computed stabilized

Table 1 — Second-order perturbation theory analysis of Fock matrix in NBO basis for 5H1MX

Donor	Type	ED/e( $q_i$ )	Acceptor	Type	ED/e( $q_j$ )	kcal/mol	$E(j)-E(i)$ a.u.	$F(I,j)$ a.u.
C 13 - C 17	$\pi^*$	0.36202	C 12 - C 15	$\pi^*$	0.31736	472.42	0.02	0.149
C 12 - H 20	$\sigma$	1.97716	C 13 - C 17	$\sigma^*$	0.02326	462.19	0.33	0.347
O 2	LP (2)	1.90729	C 13 - C 17	$\sigma^*$	0.02326	380.46	0.09	0.169
C 17 - H 24	$\sigma$	1.97813	C 13 - C 17	$\sigma^*$	0.02326	380.26	0.38	0.34
O2	LP (1)	1.94188	C 13 - C 17	$\sigma^*$	0.02326	322.9	0.11	0.171
C 12 - H 20	$\sigma$	1.97716	C 10 - C 14	$\pi^*$	0.31675	320.95	0.19	0.238
C 12 - C 15	$\pi$	1.69592	C 18 - H 26	$\sigma^*$	0.01948	300.5	0.65	0.425
C 12 - H 20	$\sigma$	1.97716	C 18 - H 26	$\sigma^*$	0.01948	297.53	0.97	0.48
C 13 - C 17	$\pi^*$	0.36202	C 11 - C 16	$\pi^*$	0.28663	290.34	0.02	0.131
O 2 - C 10	$\sigma$	1.99052	C 10 - C 14	$\pi^*$	0.31675	272.91	0.42	0.33
O 2 - C 18	$\sigma$	1.97799	C 18 - H 26	$\sigma^*$	0.01948	263.63	1.09	0.479
C 14 - C 15	$\sigma$	1.97665	C 15 - H 22	$\sigma^*$	0.01334	239.28	0.04	0.088
C 18 - H 27	$\sigma$	1.99551	C 18 - H 26	$\sigma^*$	0.01948	239.15	0.83	0.399
O 2 - C 18	$\sigma$	1.97799	C 10 - C 14	$\pi^*$	0.31675	233.87	0.31	0.26
O 2 - C 10	$\sigma$	1.99052	C 13 - C 17	$\sigma^*$	0.02326	225.2	0.56	0.319
C 17 - H 24	$\sigma$	1.99551	C 10 - C 14	$\pi^*$	0.31675	217.14	0.24	0.222
C 13 - C 17	$\pi^*$	0.36202	C 18 - H 26	$\sigma^*$	0.01948	215.29	0.52	0.683
O 3	LP (1)	1.97854	C 10 - C 14	$\pi^*$	0.31675	165.01	0.22	0.185
C 11 - C 16	$\pi^*$	0.28663	C 18 - H 26	$\sigma^*$	0.01948	146.65	0.49	0.615
C 10 - C 14	$\sigma$	1.97793	C 10 - C 14	$\pi^*$	0.31675	146.55	0.25	0.187
C 14 - H 21	$\sigma$	1.97677	C 18 - H 26	$\sigma^*$	0.01948	133.5	0.87	0.304
C 12 - C 15	$\pi^*$	0.31736	C 13 - C 17	$\pi^*$	0.36202	128.34	0.13	0.117
C 5 - C 10	$\sigma$	1.97153	C 10 - C 14	$\pi^*$	0.31675	118.61	0.24	0.164
C 18 - H 26	$\sigma$	1.99511	C 12 - H 20	$\sigma^*$	0.01316	116.88	0.59	0.234
C 16 - H 23	$\sigma$	1.98074	C 13 - C 17	$\sigma^*$	0.02326	115.7	0.2	0.137
C 10 - C 14	$\sigma$	1.97793	C 15 - H 22	$\sigma^*$	0.01334	112.69	0.05	0.065
C 10 - C 14	$\pi^*$	0.31675	C 18 - H 26	$\sigma^*$	0.01948	108.61	0.78	0.634
C 18 - H 27	$\sigma$	1.99551	C 12 - H 20	$\sigma^*$	0.01316	108.12	0.59	0.225
O 2 - C 18	$\sigma$	1.97799	C 12 - H 20	$\sigma^*$	0.01316	107.03	0.85	0.27
C 12 - C 15	$\pi^*$	0.31736	C 11 - C 16	$\pi^*$	0.28663	106.06	0.15	0.115
C 12 - C 15	$\pi^*$	0.31736	C 18 - H 26	$\sigma^*$	0.01948	100.06	0.5	0.486
C 18 - H 26	$\sigma$	1.99511	C 12 - C 15	$\pi^*$	0.31736	97.9	0.33	0.175
C 18 - H 27	$\sigma$	1.99551	C 12 - C 15	$\pi^*$	0.31736	96.03	0.33	0.173
C 12 - H 20	$\sigma$	1.97716	C 12 - H 20	$\sigma^*$	0.01316	91.58	0.73	0.231

energies between the 5H1MX's donor and acceptor pairs. The calculated stabilized energies between the donor and acceptor pairs of the 5H1MX are shown in (Table 1). Interaction C13-C17\* to C12-C15\* was determined to possess the highest stabilization energy which is 472.42 kcal/mol. An elevated E2 NBO analysis discloses a scheme with a high amount of recombination and an energetic interchange involving both donor and acceptor electrons. Other notable exchanges include C 12- H 20 to C 12- H20\*, which has a lowermost stabilization energy of 91.58 kcal/mol<sup>21,22</sup>.

#### Fukui functions

The population-based Fukui function provides quantitative information about the reactivity of individual atoms, including their nucleophilicity and electrophilicity<sup>23,24</sup>. Electron density differs with the number of electrons that are present at a certain

region. The Fukui function involves adding or subtracting electrons from the molecule. Use this function to determine the reactivity of 5H1MX with various compounds. Fukui function, which determines local softness, may be utilized during biological studies to analyse ligand and protein docking. Exact charges of the Fukui function are derived via Mulliken population analysis<sup>25,26</sup>. The atom is being attacked electrophilically if  $f(r)$  is negative or nucleophilically if  $f(r)$  is positive. Each atom is included in Table 2 along with its Dual and function descriptions. The value of the atom 9C is the lowest (-0.124), and the value of the atom 14C is the greatest (+0.075). The dual descriptor ordering for positive values is 14C > 18C > 10 > 6C > 4O > 16C > 12C > 2O > 19H > 25H, 23H > 13C > 7C > 5C, and 21H > 20H. The negative  $f(r)$  is arranged in the following manner of 9°C, 3°C, >15°C, 10°C, 27°H, 26°H, 28°H, 22°H, and 11°C, 24°H.

Table 2 — Condensed Fukui function, local softness, and dual descriptor of 5H1MX

Atom	Mulliken atomic charges			Fukui functions			dual des	local softness		
	0, 1 (N)	N+1 (-1, 2)	N-1 (1,2)	$f_r^+$	$f_r^-$	$f_r^0$	delta fr	sr+ $f_r^+$	sr- $f_r^-$	sr0 $f_r^0$
1 O	-0.0069	0.082079	-0.05563	0.089	0.049	0.069	0.04	0.019	0.011	0.015
2 O	-0.1151	-0.075285	-0.1378	0.04	0.023	0.031	0.017	0.009	0.005	0.007
3 O	-0.2626	-0.202601	-0.39386	0.06	0.131	0.096	-0.071	0.013	0.029	0.021
4 O	-0.2254	-0.158691	-0.2551	0.067	0.03	0.048	0.037	0.015	0.006	0.011
5 C	1.05287	1.094466	1.013845	0.042	0.039	0.04	0.003	0.009	0.009	0.009
6 C	1.17317	1.224589	1.160879	0.051	0.012	0.032	0.039	0.011	0.003	0.007
7 C	-0.8394	-0.869292	-0.80553	-0.03	-0.034	-0.032	0.004	0.007	-0.007	-0.007
8 C	-1.483	-1.516936	-1.40535	-0.034	-0.078	-0.056	0.044	0.007	-0.017	-0.012
9 C	-0.1403	-0.129837	-0.27454	0.01	0.134	0.072	-0.124	0.002	0.029	0.016
10 C	-0.0957	-0.051684	-0.1709	0.044	0.075	0.06	-0.031	0.01	0.016	0.013
11 C	0.56656	0.64548	0.483074	0.079	0.083	0.081	-0.005	0.017	0.018	0.018
12 C	-0.5945	-0.558113	-0.60593	0.036	0.011	0.024	0.025	0.008	0.002	0.005
13 C	-0.2908	-0.280771	-0.29602	0.01	0.005	0.008	0.005	0.002	0.001	0.002
14 C	0.23134	0.311801	0.225593	0.08	0.006	0.043	0.075	0.018	0.001	0.009
15 C	-0.2159	-0.240353	-0.26168	-0.024	0.046	0.011	-0.07	0.005	0.01	0.002
16 C	-0.2492	-0.211045	-0.25298	0.038	0.004	0.021	0.034	0.008	0.001	0.005
17 C	0.00298	0.02115	-0.07959	0.018	0.083	0.05	-0.064	0.004	0.018	0.011
18 C	-0.292	-0.301411	-0.23114	-0.009	-0.061	-0.035	0.051	0.002	-0.013	-0.008
19 H	0.18962	0.23553	0.158778	0.046	0.031	0.038	0.015	0.01	0.007	0.008
20 H	0.18689	0.238623	0.135418	0.052	0.051	0.052	0	0.011	0.011	0.011
21 H	0.19287	0.252586	0.136302	0.06	0.057	0.058	0.003	0.013	0.012	0.013
22 H	0.17991	0.233593	0.119124	0.054	0.061	0.057	-0.007	0.012	0.013	0.012
23 H	0.17612	0.239542	0.120675	0.063	0.055	0.059	0.008	0.014	0.012	0.013
24 H	0.13466	0.19052	0.077096	0.056	0.058	0.057	-0.002	0.012	0.013	0.012
25 H	0.26704	0.297947	0.244507	0.031	0.023	0.027	0.008	0.007	0.005	0.006
26 H	0.17469	0.18101	0.15848	0.006	0.016	0.011	-0.01	0.001	0.004	0.002
27 H	0.11955	0.144706	0.077014	0.025	0.043	0.034	-0.017	0.005	0.009	0.007
28 H	0.16267	0.202397	0.115267	0.04	0.047	0.044	-0.008	0.009	0.01	0.009

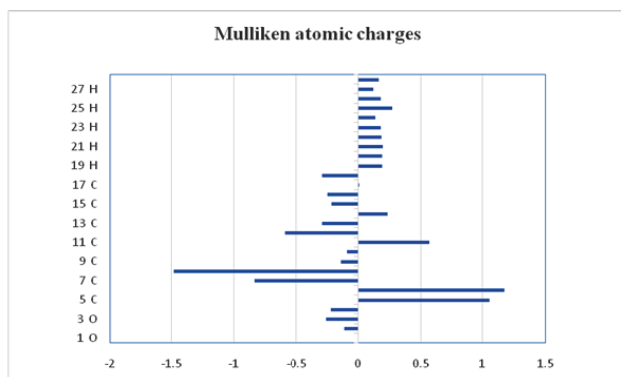


Fig. 2 — Mulliken atomic charges of 5H1MX

Table 3 — Mulliken atomic charges of 5H1MX

Atom	Mulliken atomic charges	Atom	Mulliken atomic charges
1 O	-0.007	15 C	-0.216
2 O	-0.115	16 C	-0.249
3 O	-0.263	17 C	0.003
4 O	-0.225	18 C	-0.292
5 C	1.053	19 H	0.190
6 C	1.173	20 H	0.187
7 C	-0.839	21 H	0.193
8 C	-1.483	22 H	0.180
9 C	-0.140	23 H	0.176
10 C	-0.096	24 H	0.135
11 C	0.567	25 H	0.267
12 C	-0.595	26 H	0.175
13 C	-0.291	27 H	0.120
14 C	0.231	28 H	0.163

#### Mulliken charge studies

The estimation of Mulliken charge distribution for 5H1MX was carried out and (Fig. 2) shows the graphical representation. The Mulliken charge distribution reveals significant variation in charge among the 28 atoms of 5H1MX. 6C carries the highest positive charge of 1.173167. Carbon has a higher local electronegative charge than any other atom, giving 5C the second-highest positive charge (1.052874). Positive charges are present on all other carbon atoms (0.231344, 0.002982). It has been established that hydrogen molecules only possess positive charges and that oxygen molecules possess just negative charges shown in (Table 3).

#### MEP analysis

The MEP calculation of the 5H1MX molecule is displayed in (Fig. 3) along with the colour-graded maps. The MEP analysis, which depends on many factors like dipole moment and the density of electrons, indicates the type of chemical attack that may occur at all the different reactive sites inside the molecule under investigation<sup>27</sup>. The developed

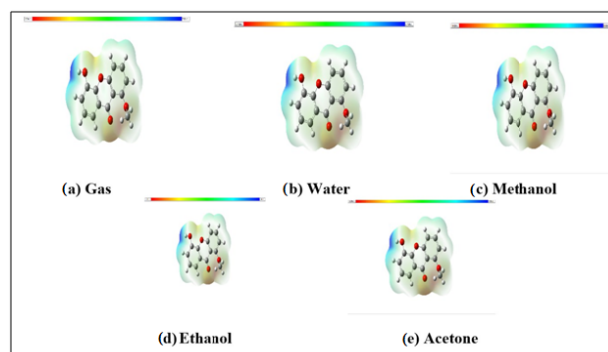


Fig. 3 — MEP maps of the 5H1MX compound in gas and green solvent

electrostatic potential is calculated over a surface having a uniform electron density on which the Mep map is built<sup>28</sup>. According to this system of color grading, nucleophiles prefer blue regions while electrophilic reagents are most likely to attack red sections. Upon solvation, there is no discernible change in color gradation. However, the medium's polarity increases during solvation and the electrostatic potential range expands significantly. As a result, the potential range expands from  $-7.000 \times 10^{-2}$  a.u. to  $7.000 \times 10^{-2}$  a.u. (atomic unit is referred to as a.u.) in the gaseous phase,  $8.472 \times 10^{-2}$  a.u. to  $8.472 \times 10^{-2}$  a.u. in water,  $8.425 \times 10^{-2}$  a.u. to  $8.425 \times 10^{-2}$  a.u. in methanol,  $8.401 \times 10^{-2}$  a.u. and  $8.401 \times 10^{-2}$  a.u. in ethanol and  $-8.380 \times 10^{-2}$  a.u. to  $8.380 \times 10^{-2}$  in acetone. Finally, it demonstrates that the water solvent's polarity gradient is higher. Therefore, when the polarity of the solvents rises, the molecules exhibit a larger potential range, suggesting that they would interact with solvation in a more polar (charged) manner and a compound's bioactivity may be anticipated based on the MEP map<sup>29</sup>. The intermolecular interactions controlling the stability and reactivity of the 5H1MX molecule are better understood thanks to the electronic characteristics derived from NBO, MEP, and Fukui function investigations. Strong donor-acceptor interactions, which greatly enhance molecule stability, are indicated by the high stabilization energy found in NBO analysis. Electron-rich and electron-deficient areas that are vulnerable to electrophilic and nucleophilic assaults, respectively, are further identified by the MEP surface. Additionally, RDG–NCI analysis verifies that the molecular framework contains weak non-covalent interactions such steric repulsions and van der Waals forces. These interactions affect the molecule's binding affinity toward biological targets and are essential in

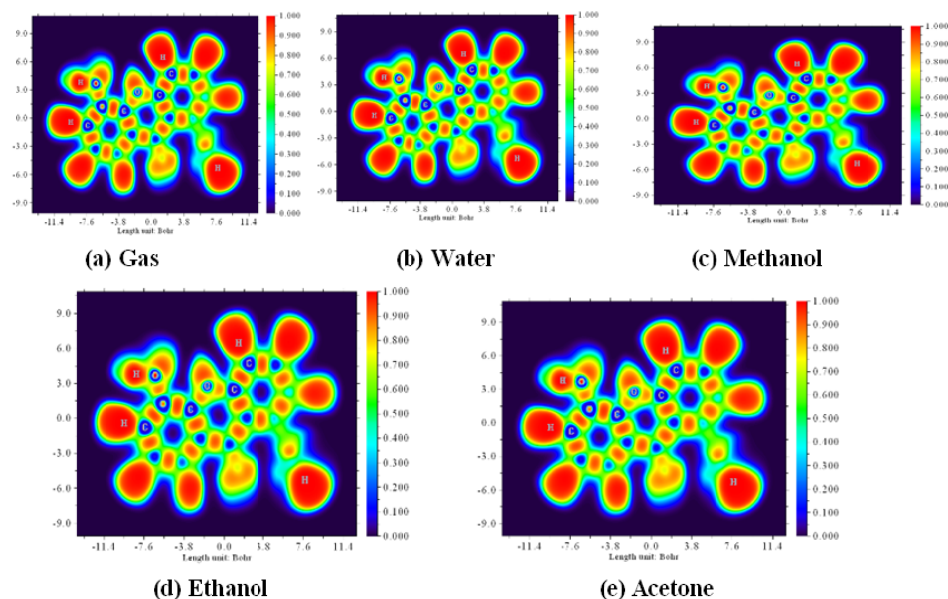


Fig. 4 — ELF colour-filled maps of the 5H1MX molecule in gas and different solvents

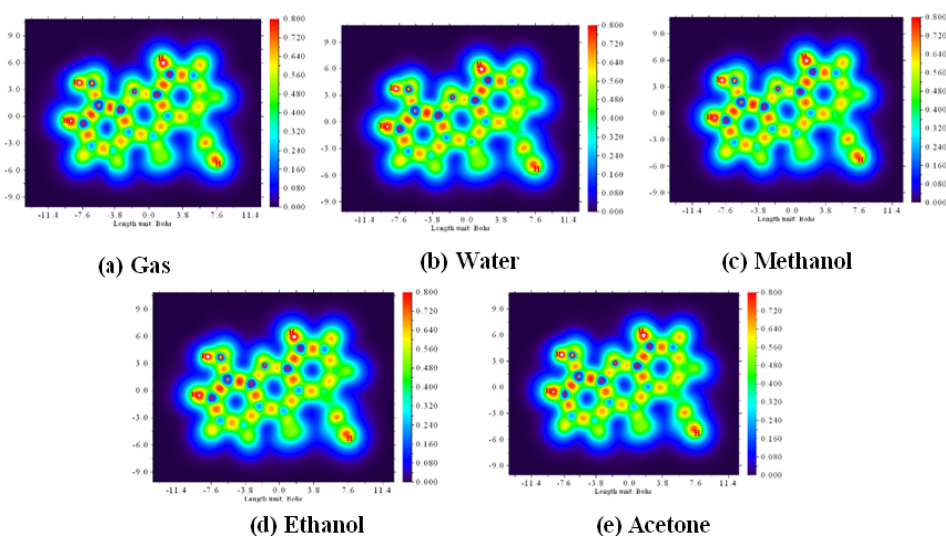


Fig. 5 — LOL colour-filled maps of the 5H1MX molecule in gas and different solvents

determining the overall structural stability. Thus, a clear connection between molecule structure, stability, and biological activity is established by combining the interpretation of electronic descriptors with interaction analysis.

#### ELF and LOL analysis

The strength of Pauli repulsion between molecular orbitals is predicted by the Electron Localised Function analysis (ELF). Illustrations of the ELF emission in gas and solvents are shown in (Fig. 4)<sup>30</sup>. Hydrogen 1s orbitals are extremely tiny, and molecular aromatic hydrogens have an abundance of red regions, which means that substantial Pauli

repulsion is occurring there. The bluish regions are the higher 2s and 3s orbitals of oxygen and aromatic carbons that are concentrated since there is less Pauli repulsion in these locations. However, Pauli repulsion increases as orbital electrons become closer as well as suffer repulsion on engagement such that reddish patches can be detected in the bonded orbital overlay around aromatic carbons. In various solvent media, Pauli repulsion does not appear to fluctuate<sup>31</sup>.

The depth of pi-orbital delocalization over a complete biological system is shown by the Localised Orbital Locator (LOL) research. The LOL output photos in various media are shown in (Fig. 5). As the

density of electrons overflows the top edge and the core of the hydrogen atom has a higher LOL value in the covalent region, it indicates red. The position of electron reduction via valence to its inner shell is indicated through a bluish circle.

#### RDG -NCI analysis

A distinctive technique for predicting and illustrating the strongest molecular connections is the Reduced Density Gradient which can be calculated using Atomistica online tool and VMD software<sup>32</sup>. A hydrogen bond forms such that green denotes a Wander-Waals interaction and red denotes steric repellent interactions as shown in (Fig. 6). For weak connection projections, sign  $(\lambda_2)\rho$  (a.u.) ranging from -0.04 to 0.04 in RDG maps have been obtained in many solvents including gas, water, methanol, ethanol, and acetone. The elliptical red plate at the aromatic ring hub is connected to phenyl rings and has a significant steric impact because of strong repellent forces<sup>33,34</sup>. Red-green spotted flaky zone from 0.00 to 0.01 a.u. displays the C-H connections denoting a weak Vander Waals force of contact, and a low electron density. There are no significant NCI or H-bonds between the phenyl rings, according to RDG evaluation, because there are no blue spikes between

0.01 and 0.04 a.u. In addition, a blue-ringed area that is scattered across the picture indicates the presence of an H-bond inside the molecular structure. Due to the effects of the solvent, 5H1MX does not significantly change in the case of RDG.

#### Drug likeness

The compound 5-Hydroxy-1-Methoxyxanthone ( $C_{14}H_{10}O_4$ ) has attracted interest because of its possible anti-diabetic properties. The assessment of the drug's safety profile, mechanism of action, and efficacy is part of the pharmacological inquiry. Criteria for drug-likeness activity can be predicted by the Lipinski rule of five<sup>35</sup>, if it will have strong drug-like qualities and be an excellent option for a drug. In the current investigation, the overall score value of a drug's likeness is calculated. The criteria measuring the compound's drug-likeness are compiled in (Table 4). The Swiss ADME program may be used in this way to carry out a range of tasks<sup>36,37</sup>. The set of criteria put forward by Lipinski<sup>38</sup> is in favour of this result. It is assured to adhere to the drug rules, therefore there are no violations. The molecular weight is 242.23 g/mol, with HBD (Donor) = 1, and HBA (Acceptor) = 4. Lipophilicity is a vital physical-chemical factor for defining drug similarity.

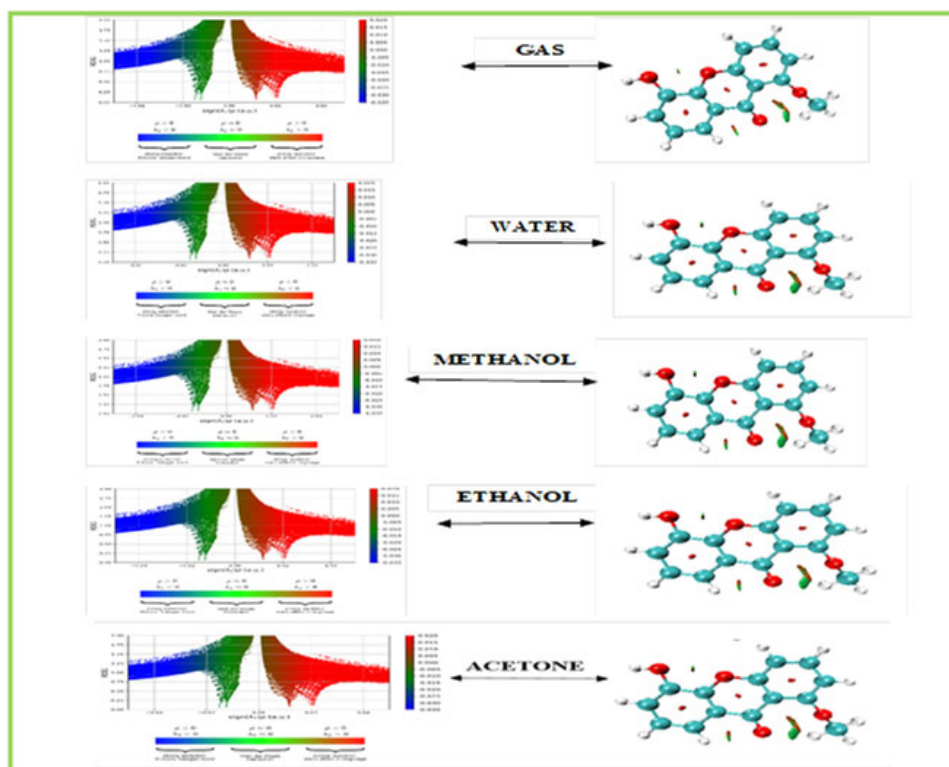


Fig. 6 — RDG and NCI analysis of the 5H1MX molecule in gas and different solvents

Table 4 — Drug discovery parameters for 5H1MX	
Descriptor	Value
<i>Physicochemical properties</i>	
Hydrogen Bond Donor (HBD)	1
Hydrogen Bond Acceptor (HBA)	4
AlogP	0
Topological polar surface area (TPSA)	59.67 Å <sup>2</sup>
Molar refractivity	68.51
Number of atoms	28
Number of rotatable bonds	1
<i>Lipophilicity</i>	
iLOGP	2.14
XLOGP	2.58
WLOGP	2.66
MLOGP	1.13
SILICOS-IT	2.98
Consensus LOGP	2.30
<i>Water Solubility</i>	
LogS(ESOL)	-3.48
<i>Pharmacokinetics</i>	
GI absorption	High
Log Kp (skin permeation)	-5.95 cm/s
<i>Druglikeness</i>	
Lipinski	Yes, 0 violation
Veber	Yes
Bioavailability Score	0.55
<i>Medicinal Chemistry</i>	
Leadlikeness	No;1 violation: MW<250
Synthetic accessibility	2.95

Therefore, it is evident that the title compound accurately describes the characteristics necessary for the chemical to function as a drug. It is obvious from this that the chemical's name appropriately captures the qualities necessary for the drug to serve as a treatment. These findings demonstrate that the chemical is bioactive<sup>39</sup>.

### Molecular docking

The molecular docking method is now often employed in biological research for the creation of new drugs. The 5H1MX molecule has a strong anti-diabetic effect, the target protein (PDB ID: 3CV7) associated with diabetes was obtained from the Protein Data Bank (RCSB)<sup>40</sup>. This work attempts to evaluate the binding affinity of 5-Hydroxy-1-Methoxyxanthone to target proteins and its possible effect on glucose metabolism by combining computational predictions with experimental data. It is anticipated that the outcomes of these investigations will offer significant perspectives on the medicinal possibilities of this substance and its function in the control of diabetes. To acquire the rank one value at

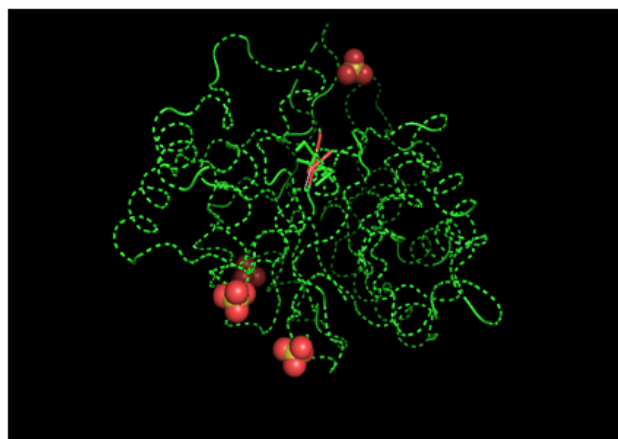


Fig. 7 — Molecular docking with 3cv7 protein



Fig. 8 — 3D diagram of Molecular docking with 3cv7 protein

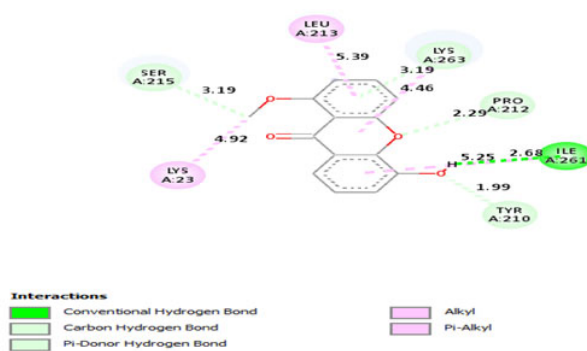


Fig. 9 — 2D diagram of Molecular docking with 3cv7 protein

the lowest feasible cost, as shown in (Fig. 7), the 5H1MX molecule was docked into the active site of the target protein. Molecular docking binding energies (kcal/mol), bond lengths, and the number of residues is provided in (Table 5). Figure 8 shows a 3D depiction of the docked position of 3cv7. The two-dimensional model is shown in (Fig. 9). The low binding energy of the protein 3cv7, which is -7.14

Table 5 Molecular docking with antidiabetic's protein of 5H1MX

Protein (PDB ID)	Residue	Type of Interactions	Bond dist. (Å)	Binding energy (Kcal/mol)	Estimated inhibition constant (micromolar)	Inter molecular energy (Kcal/mol)	vdW + H bond + dissolve Energy (kcal/mol)	Reference RMSD (Å)
	LEU A-213	Alkyl	5.39	-7.14	5.88	-7.73	-7.65	27.95
	LYS A-23	Pi- Alkyl	4.92					
	SER A-215	Carbon	3.19					
3cv7		H- Bond						
	LYS A-263	Carbon	3.19					
		H- Bond						
	PRO A- 212	Pi-Donor	2.29					
		H- Bond						
	TYR A-210	Pi-Donor	1.99					
		H- Bond						

kcal/mol, makes it suitable for biological activity<sup>41,42</sup>. This chemical is recommended as a possible diabetes treatment since it has strong protein binding with 3cv7 and a low binding energy value<sup>43</sup>.

### Conclusion

The current work verifies the structural and electronic characteristics of 5H1MX using a combination of experimental and theoretical methodologies. Strong donor-acceptor contacts with high stabilization energy were found by NBO analysis, suggesting molecular stability. While ELF, LOL, and RDG investigations shed light on electron localization and intermolecular interactions, MEP and Fukui analysis indicated important reactive sites. The chemical demonstrated significant binding affinity (-7.14 kcal/mol) for the target protein and excellent drug-likeness characteristics. These results imply that 5H1MX is a good option for the development of antidiabetic medications.

### Conflict of interest

All authors declare no conflict of interest.

### References

- Quillinan AJ & Scheinmann F, Extractives from Guttiferae Part XXV Synthesis of the natural 1, 5-dioxygenated xanthenes, dehydrocycloguanandin, guanandin, isoguanandin, and 5-hydroxy-1-methoxyxanthone. *J Chem Soc Perkin Trans*, 1 (1972) 1382.
- Rocha L, Andrew M, Auxiliadora M, Kaplan C, Stoeckli-Evans H, Thull U, Bernard T & Kurt H, An antifungal  $\gamma$ -pyrone and xanthenes with monoamine oxidase inhibitory activity from *Hypericum brasiliense*. *Phytochem*, 36 (1994) 6 1381.
- Lee KH, Chai HB, Tamez PA, Pezzuto JM, Geoffrey A Cordell, Win KK & Maung TW, Biologically active alkylated coumarins from *Kayea assamica*. *Phytochemistry*, 64 (2003) 535.
- Hideki T, Munekazu I, Murakami KI, Tetsuro I, Toshiyuki T, Veliah C & Soedarsono R, Three xanthenes from *Poeciloneuron pauciflorum* and *Mammea acuminata*. *Phytochemistry*, 45 (1997) 133.
- Prapaporn C, Arnon C, Apirak P, Arisara P, Tachpon T, Walaiporn P & Chuchard P, Antimalarial potential of compounds isolated from *Mammeasiamensis* T. Anders. flowers: in vitro and molecular docking studies. *BMC Complement Med Ther*, 22 (2022) 1.
- Zhou, Guan S, Xiao JY, Yong J & Peng FT, Flavanoids and xanthenes isolated from *Arenaria serpyllifolia* L. *J Chin Pharm Sci*, 22 (2013) 286.
- Rifat R, Ahmed S & Hassan MM, *Arenaria serpyllifolia* L.: a review of medicinal uses, phytochemistry and pharmacology. *WJPPS*, 10 (2021) 157.
- Avdovi EH, Dimi DS, Fronc M, Kožišek J, Klein E, Milanovi ZB, Kesi K & Markovi ZK, Structural and theoretical analysis, molecular docking/dynamics investigation of 3-(1-m-chloridoethylidene)-chromane-2,4-dione: the role of chlorine atom. *J Mol Struct*, 1231 (2021) 129962.
- Laura JJ, Rajesh P, Kesavan M, Dhanalakshmi E, Kayashrini S & Prabhakaran M, Degree-based topological indices, NMR chemical shifts, chemical reactivity, molecular dynamics and DFT analysis of 1, 4-Methanoazulene-9-methanol, Decahydro-4, 8, 8-trimethyl-, [1S-(1 $\alpha$ , 3 $\beta$ , 4 $\alpha$ , 8 $\alpha\beta$ , 9R)]. *Biophys Chem*, 322 (2025) 107442.
- Medimagh M, Issaoui N, Gatfaoui S, Kazachenko AS, Al-Dossary OM, Kumar N & Bousiakoug LG, Investigations on the non-covalent interactions, drug-likeness, molecular docking and chemical properties of 1, 1, 4, 7, 7-pentamethyldiethylenetriammonium trinitrate by density-functional theory. *J King Saud Univ-Sci*, 35 (2023) 102645.
- Manaa MB, Issaoui N, Bouaziz N & Lamine AB, Combined statistical physics models and DFT theory to study the adsorption process of paprika dye on TiO<sub>2</sub> for dye sensitized solar cells. *J Mater Res Technol*, 9 (2020) 1175.
- Revathi G, Rajesh P, Kayashrini S & Abirami SB, Investigation of Bioactive Properties, Structural, Electronic, Reactivity Analysis and Quantum-Based Characterization of Hexadecanamide. *Silico Res Biomed*, (2026) 100287.
- Frisch MJ, Trucks GW, Schlegel HB, Scuseria GE, Robb MA, Cheeseman JR, Scalmani G, Barone V, Mennucci B, Petersson GA, Nakatsuji H, Caricato M, Li X, Hratchian HP, Izmaylov AF, Bloino J, Zheng G, Sonnenberg JL, Hada M, Ehara M, Toyota K, Fukuda R, Hasegawa J, Ishida M, Nakajima T, Honda Y, Kitao O, Nakai H, Vreven T, Montgomery JA, Peralta JE, Ogliaro F,

- Bearpark M, Heyd JJ, Brothers E, Kudin KN, Staroverov VN, Kobayashi R, Normand J, Raghavachari K, Rendell A, Burant JC, Iyengar SS, Tomasi J, Cossi M, Rega N, Millam JM, Klene M, Knox JE, Cross JB, Bakken V, Adamo C, Jaramillo J, Gomperts R, Stratmann RE, Yazyev O, Austin AJ, Cammi R, Pomelli C, Ochterski JW, Martin RL, Morokuma K, Zakrzewski VG, Voth GA, Salvador P, Dannenberg JJ, Dapprich S, Daniels AD, Farkas O, Foresman JB, Ortiz JV, Cioslowski J & Fox DJ. Gaussian 09 Revision A.1, Gaussian Inc., Wallingford, CT, 2009
- 14 Dennington RD, Keith TA & Millam JM, Gauss View, Version 5.0, Semichem Inc., Shawnee Mission KS, 2009.
- 15 Lawrence M, Paulraj EI & Rajesh P, Spectroscopic characterization, electronic transitions and pharmacodynamic analysis of 1-Phenyl-1, 3-butanedione: An effective agent for antipsychotic activity. *Chem Phys Impact*, 6 (2023) 100226.
- 16 Morris GM, AutoDock 4 and AutoDockTools 4: automated docking with selective receptor flexibility. *J Comput Chem*, 30 (2009) 2785.
- 17 The PyMOL Molecular Graphics Development Component, Version 1.8, PYMOL Mol. Graph. Dev. Component, Version 1.8, Schrodingier LLC.
- 18 Laura JJ, Rajesh P, Kayashrini S & Abirami SB, Kojibiose as a Sustainable Bioactive Molecule: Experimental and DFT Insights into Antibacterial Activity and Electronic Properties. *J. Mol. Struct*, (2026) 145576.
- 19 Rekha S, Tamilselvan S, Vetrivelan V, Mishma JNC, Kadaikunnan S, Abbas G & Muthu S, Effect of different solvents, molecular level vibrational energies, electronic, electrostatic, donar-acceptor and pharmaceutical studies on 3-Methoxy phenyl acetonitrile-anti depressant agent. *J Mol Liq*, 1016 (2023)122308.
- 20 Kayashrini S, Rajesh P, Kesavan M, Kala A & Pavithra M, Application of Degree-Based Topological Descriptors, Molecular Properties, Chemical Reactivity Prediction and Nonlinear Optical Analysis of 5-[2-[4-(1, 2-benzothiazol-3-yl) piperazin-1-yl] ethyl]-6-chloro-1, 3-dihydroindol-2-one. *J Mol Struct*, (2025) 144847.
- 21 Fukui K, A study of correlation of the order of chemical reactivity of a sequence of binary compounds of nitrogen and oxygen in terms of frontier orbital theory, *Curr Sci*, 218 (1982) 747.
- 22 Lawrence M, Rajesh P, Ahmad Irfan & Muthu S, Importance of solvent roles in molecular, electronic and dynamical properties, thermodynamic quantities, Mulliken charges, reactive analysis and molecular docking of 2-Bromo-1H-imidazole-4,5-dicarbonitrile. *J Mol Liq*, 388 (2023) 122744.
- 23 Sumithra M, Sundaraganesan N, Rajesh R, Ilangovan V, Irfan a & Muthu S, Electron density, charge transfer, solvent effect and molecular spectroscopic studies on 2, 2-Dimethyl-N-pyridin-4-yl-propionamide-A potential antioxidant. *Comput Theor Chem*, 1223 (2023) 114103.
- 24 Mohamed y, Insights into structural, solvent effect, molecular properties and NLO behavior of hemithioindigo-photoisomerization: a DFT study. *J Mol Liq*, 342 (2021) 116944.
- 25 Kayashrini S, Rajesh P, Dhanalakshmi E, Kesavan M, Prabhakaran M, Al Farraj DA & Elshikh MS, FT-IR, UV-Vis, density functional theory and molecular docking studies on 3, 7, 11, 15-Tetramethyl-2hexadecen-1-ol. *J Mol Struct*, 1321 (2025) 139600.
- 26 Akman F, A comparative study based on molecular structure, spectroscopic, electronic, thermodynamic and NBO analysis of some nitrogen-containing monomers. *Polym Bull*, 78 (2021) 663.
- 27 Demircioglu Z, Kas tas CA & Büyükgüngör O, Theoretical analysis (NBO, NPA, Mulliken Population Method) and molecular orbital studies (hardness, chemical potential, electrophilicity and Fukui function analysis) of (E)-2-((4-hydroxy-2- methylphenylimino) methyl)-3-methoxyphenol. *J Mol Struct*, 1091 (2015) 183.
- 28 Gatfaoui S, Issaoui N, Mezni A, Bardak F, Roisnel T, Atac A & Marouani H, Synthesis, structural and spectroscopic features, and investigation of bioactive nature of a novel organic-inorganic hybrid material 1H-1, 2, 4-triazole-4-ium trioxonitrate. *J Mol Struct*, 1150 (2017) 242.
- 29 Khodiev M, Holikulov U, Jumabaev A, Issaoui N, Lvovich LN, Al-Dossary OM & Bousiakoug LG. Solvent effect on the self-association of the 1, 2, 4-triazole: A DFT study. *J Mol Liq*, 382 (2023) 121960.
- 30 Ramalingam A, Mustafa N, Chng WJ, Medimagh M, Sambandam S & Issaoui N, 3-Chloro-3-methyl-2, 6-diarylpiperidin-4-ones as anti-cancer agents: synthesis, biological evaluation, molecular docking, and *in silico* ADMET prediction. *Biomol*, 12 (2022) 1093.
- 31 Kazachenko AS, Vasileva NY, Fetisova OY, Sychev VV, Elsufov EV, Malyar YN & Ionin VA, New reactions of betulin with sulfamic acid and ammonium sulfamate in the presence of solid catalysts. *Biomass Convers Biorefin*, 14 (2024) 4245.
- 32 Pavia JR, Lampman GM & Kriz GS, Introduction to Spectroscopy, fourth ed., Brooks/Cole, Belmont, USA, (2009).
- 33 Andrew F Parsons, Keynotes in Organic Chemistry. *Blackwell Publishing*, Oxford, UK, (2003) ISBN-0632058161.
- 34 Cousins KR, Computer review of ChemDraw Ultra 12.0. *J Am Chem Soc*, 11 (2011) 133 21 8388.
- 35 Daina A, Michielin O & Zoete V, SwissADME: a free web tool to evaluate pharmacokinetics, druglikeness and medicinal chemistry friendliness of small molecules. *Sci Rep*, 7 (2017) 42717.
- 36 Issaoui N, Ghalla H, Bardak F, Karabacak M, Aouled DN, Flakus HT & Oujia B, Combined experimental and theoretical studies on the molecular structures, spectroscopy, and inhibitor activity of 3-(2-thienyl) acrylic acid through AIM, NBO, FT-IR, FT-Raman, UV and HOMO-LUMO analyses, and molecular docking. *J Mol Struct*, 1130 (2017) 659.
- 37 Helen MB, Westbrook J, Feng Z, Gilliland G, Bhat TN, Weissig H, Shindyalov IN & Philip E, Bourne, The protein data bank. *Nucleic Acids Res*, 28 (2000) 235.
- 38 Lawrence M, Rajesh P & Sahaya Jude Dhas S, Quantum chemical calculation and spectroscopic approach for the analyses of 2-oxovaleric acid, methyl ester. *J Pharm Negat*, 13 (2023) 1495.
- 39 Agarwal N, Verma I, Siddiqui N & Javed S, Experimental spectroscopic and quantum computational analysis of pyridine-2, 6-dicarboxylic acid with molecular docking studies. *J Mol Struct*, 1245 (2021) 131046.
- 40 Al-Otaibi JS, Mary YS, Mary YS, Nivedita A, Balachandar S & Yathirajan HS, Insights into solvation effects,

- spectroscopic, Hirshfeld surface Analysis, reactivity analysis and anti-COVID-19 ability of doxylamine succinate: experimental, DFT, MD and docking simulations. *J Mol Liq*, 361 (2022) 119609.
- 41 Sathya B, Prasath M & Muthu S, Spectroscopic investigations, quantum chemical calculations and molecular docking studies of Mangiferin - an anti-viral agent of H1N1 Influenza virus. *Chem Data Collect*, 30 (2020) 100580.
- 42 Pallavi HM, Fares H, Al O, Vivek HK & Shaukath A, Synthesis, characterization, DFT, docking studies and molecular dynamics of some 3-phenyl- 5-furan isoxazole derivatives as anti-inflammatory and anti-ulcer agents. *J Mol Struct*, 1250 (2022) 131812.
- 43 Ramaiah K, Koya Pr, Rao G, Naresh R & Jyothi P, Zinc (II) complex: spectroscopic, physicochemical calculations, anti-inflammatory and *in silico* molecular docking studies. *J Mol Struct*, 1263 (2022) 133070.